Applied Physics Express

LETTER • **OPEN ACCESS**

Rejuvenation of degraded Zener diodes with the electron wind force

To cite this article: Md Hafijur Rahman *et al* 2024 *Appl. Phys. Express* **17** 047001

OPEN ACCESS

Applied Physics Express 17, 047001 (2024) LETTER

https://doi.org/10.35848/1882-0786/ad379c

Rejuvenation of degraded Zener diodes with the electron wind force

Md Hafijur Rahman[1], Nahid Sultan Al-Mamun[1], Nicholas Glavin[2], Aman Haque[1*], Fan Ren[3], Stephen Pearton[4], and Douglas E. Wolfe[5]

[1]Department of Mechanical Engineering, The Pennsylvania State University, University Park, PA 16803, United States of America
[2]Air Force Research Laboratory, Materials and Manufacturing Directorate, Wright-Patterson AFB OH 45433, United States of America
[3]Chemical Engineering, University of Florida, Gainesville, FL 32611, United States of America
[4]Material Science and Engineering, University of Florida, Gainesville, FL 32611, United States of America
[5]Materials Science and Engineering Department, The Pennsylvania State University, University Park, PA 16802, United States of America

*E-mail: mah37@psu.edu

Received February 5, 2024; revised March 20, 2024; accepted March 25, 2024; published online April 17, 2024

In this study, we explore the rejuvenation of a Zener diode degraded by high electrical stress, leading to a leftward shift, and broadening of the Zener breakdown voltage knee, alongside a 57% reduction in forward current. We employed a non-thermal annealing method involving high-density electric pulses with short pulse width and low frequency. The annealing process took <30 s at near-ambient temperature. Raman spectroscopy supports the electrical characterization, showing enhancement in crystallinity to explain the restoration of the breakdown knee followed by improvement in forward current by ~85%. © 2024 The Author(s). Published on behalf of The Japan Society of Applied Physics by IOP Publishing Ltd

Zener diodes are central to various applications, ranging from voltage regulation to protection circuits.[1–3] Their fabrication processing and/or usage in harsh environments may lead to defects within the semiconductor material. It is recognized that these defects are often an inevitable consequence of material growth and processing conditions, which occur well before their integration into actual devices.[4] Both fabrication and operational stresses lead to complex defect formations, including point defects such as vacancy clusters, line defects such as dislocations, etc, which contribute to the degradation mechanisms and affect the device functionality. These intrinsic defects, originating from interfaces, surfaces, and bulk regions of the lattice,[5–7] can significantly impact the performance of semiconductor devices. The defects stem from a multitude of sources, encompassing manufacturing and materials inconsistencies, such as crystal lattice dislocations, as well as operational stressors that include but are not limited to thermal, high electrical and radiation exposure. Particularly, in the context of Zener diodes employed within high-radiation environments as a radiation sensor,[8] the defects could be attributed to radiation-induced damage, leading to the formation of point defects such as vacancy clusters and/or line defects such as dislocations. Islam et al.[9] have observed that the large fluence heavy ion radiation induces a high-density dislocation into the gallium nitride high electron mobility transistor (GaN HEMT) which degrades the device performance and reliability as the drain current decreases significantly with increasing the radiation dose. If the semiconductor contains a high density of crystal defects, the behavior of minority carriers, particularly their recombination rates, is adversely affected.[10,11] This in turn can lead to a deterioration in device functionality, especially when subjected to high electrical stress.[4] Such stress can induce additional defects within the semiconductor lattice, manifesting as trap states that elevate the ideality factor, thus deviating from the ideal behavior expected from the Shockley diode equation.[12–16]

Traditionally, thermal annealing has been used to mitigate defects to obtain improved electrical properties of semiconductor devices.[17–20] This process involves heating a material to an elevated temperature and then cooling it down. The purpose is to increase the atomic mobility within the material, which can help eliminate defects such as dislocations, vacancies, or impurities. However, in multi-layered materials with varying thermal expansion coefficients, high temperature can create thermoelastic strain during heating and cooling.[21,22] Such strain might create more defects than annihilated—increasing the overall defect density, particularly in the channels of semiconductor devices. Sub-optimal thermal annealing can therefore reduce the charge carrier mobility and diminish electronic performance. Moreover, the process is time-consuming, which may increase production costs and complexity.[23,24] This suggests the necessity for a different, ideally non-thermal method to anneal defects in electronic devices. One candidate method is electropulsing, which has been demonstrated to control defect density in metals and alloys.[25–27] We extend the concept to the semiconductor devices, recognizing that the channels and vicinity can be annealed by the effect of the electron wind force (EWF). Our recent study[28] demonstrated the rejuvenation of Ti/4H-SiC Schottky barrier diodes using high density current pulses. It is also evident that the controlled electropulsing can reduce the radiation damage of a GaN based high electron mobility transistors (HEMT).[29]

The objectives of this research are twofold: firstly, to investigate the efficacy of electropulsing treatment in reducing defect densities in a degraded Zener diode, thereby restoring their electrical characteristics; and secondly, to determine whether EPT can enhance the crystalline structure beyond the original state, as evidenced by Raman spectroscopy and electrical characterization. The scope of our inquiry encompasses both the forward and reverse bias operational modes of the diode, offering a holistic view of the rejuvenation process. We aim to address the question of whether electropulsing can serve as a feasible alternative to traditional annealing processes, offering a low-thermal-budget and time-efficient recovery method. This challenge is significant given the need for more sustainable and cost-

effective manufacturing and maintenance processes in the semiconductor industry. To do so, we first intentionally degrade the diode by applying high electrical stress which leads to a leftward shift and broadening of the Zener breakdown voltage knee, and a 57% decrease in forward current. Following that, we apply a non-thermal annealing technique which involves passing high current density pulses through the device with low duty cycles (0.04 or lower). Such a regimen ensures that thermal spikes are only transient and given ample time to dissipate, thus maintaining the processing temperature in ambient range.[30,31] The fundamental to this technique is the exploitation of the EWF, a mechanical phenomenon emanating from the momentum loss of electrons upon their interaction with lattice defects. In contrast to traditional electropulsing methods that predominantly rely on Joule heating and its associated thermal consequences,[32,33] our strategy capitalizes on the EWF to circumvent thermal effects, offering an efficient paradigm in defect mitigation and device rejuvenation. We demonstrate that the proposed electropulsing treatment effectively rejuvenated the Zener diode, restoring the breakdown knee and forward current to nearly 85% of their original states. Raman spectroscopy revealed a spatially non-uniform recovery, indicating varying effectiveness across the diode. Additionally, changes in the ideality factor further evidenced the electrical recovery, albeit with non-uniform rejuvenation.

Operational stresses such as electrical load surges and temperature fluctuations are unavoidable in some applications, degrading the functionality of Zener diodes over time, despite initial manufacturing quality. While preemptive defect mitigation during manufacturing is essential, the unpredictable nature of operational stresses necessitates robust post-degradation recovery methods. Such necessity can be seen in the use of Zener diodes as radiation sensors[8] within harsh environments. Specifically, in settings like nuclear reactors, these sensors are inevitably exposed to high levels of radiation, which can create significant defects in the devices over time.[34] Despite the best efforts in manufacturing quality control, the extreme conditions encountered in such operational scenarios can lead to the degradation of the sensors' functionality. In these cases, the ability to effectively heal the sensors using post-degradation recovery methods, such as the EWF-assisted processing explored in our study, becomes invaluable. The present study explores the EWF as a non-thermal recovery approach, emphasizing its role in enhancing the durability and performance of Zener diodes in applications where reliability is critical. This approach is supported by our previous research, which demonstrated the efficacy of EWF in mitigating post-manufacturing defects, resulting in enhanced forward current at a given voltage in pristine devices.[35] In our previous study, we have also demonstrated the efficacy of EWF assisted low-temperature processing in defect mitigation of metals and alloys.[36] Here, we extend our investigation to intentionally degraded devices, assessing EWF's effectiveness in defect mitigation within semiconductor devices, thus providing a comprehensive strategy for ensuring the longevity and reliability of these components in practical scenarios.

The experimental study was carried out on a silicon Zener diode, model (SZ3714.T), which underwent a two-stage intentional degradation process through high-electrical stress. Initially, it was subjected to a forward bias of 3 V, which significantly exceeded the manufacturer's specified maximum forward voltage of 1.1 V. The diode was maintained under this condition for an extended period of 72 h, in a controlled environment to ensure consistent application of stress. Following that, the diode was subjected to a more strenuous condition by the application of elevated Zener bias. Distinct voltage levels were chosen for this phase, such as: 16.5 V, 17 V, and 17.5 V. Each voltage was applied consecutively for a duration of 48–60 h. During each step of the degradation process, the current–voltage (I–V) characteristic curve of the diode was measured using a Keithley-2400 Source Measure Unit (SMU). Following the degradation, a controlled electropulsing treatment (pulse width 20 μs, frequency 2 Hz, time 30 s) was applied using a DC power supply (Sorensen DCS100–12E) coupled with a current pulse generator (Laser Controller, ED2P-AXA-0032). An Optris PI 640 thermal microscope was employed, allowing for the real-time observation of temperature changes during the process. Temperature profile showed less than a 10 °C increase during the annealing process, and the single pulse response indicated that the spike lasted briefly, allowing the sample ample time to dissipate heat and return to RT before the next pulse (Fig. 1). Finally, Raman spectroscopy was performed to assess the structural changes at the molecular level. The Raman spectra were obtained using a LabRAM Soleil™ Raman Microscope, which is equipped with a 50X microscopic objective lens for high-resolution imaging. For the Raman analysis, a 532 nm green laser was selected, operating at an incident power of 3.8 mW. This specific setup, including the use of an 1800 gr mm^{-1} grating, was chosen to minimize potential heating effects on the silicon structure while providing sufficient resolution to detect subtle changes in the lattice.

Figure 2 represents the I–V characteristic curves for three distinct states of the Zener diode: pristine, degraded, and after electropulsing treatment. The pristine diode's I–V curve shows the expected behavior for a Zener diode with a sharp knee indicating the breakdown voltage, at which (14.1 V) a sharp increase in current is observed. The degradation process leads to a significant deviation from the pristine behavior, particularly noticeable as a broadening of the knee (the curve flattens), and shifts to the left, suggesting a lower breakdown voltage and potentially increased leakage current before the breakdown, which are indicative of damage to the diode structure. The inset provides a focused view of the I–V characteristic curves near the knee region, from 7 to 14.5 V. It is evident from the inset that the degraded diode's breakdown voltage is significantly reduced to ~8 V. Following the electropulsing treatment, the curve for the pulsed diode shows a reversion towards the pristine state's characteristics, with a slight deviation in the knee region. The inset image shows that the breakdown voltage (~13.9 V) is sharp again and close to the pristine value (14.1 V). The similarity between the post-electropulsing and pristine curves suggests that the electropulsing treatment has effectively restored some of the diode's original electrical characteristics.

We extended our investigation to include the forward bias mode operation, which is typically less emphasized for Zener diodes but still critical for a full evaluation of diode

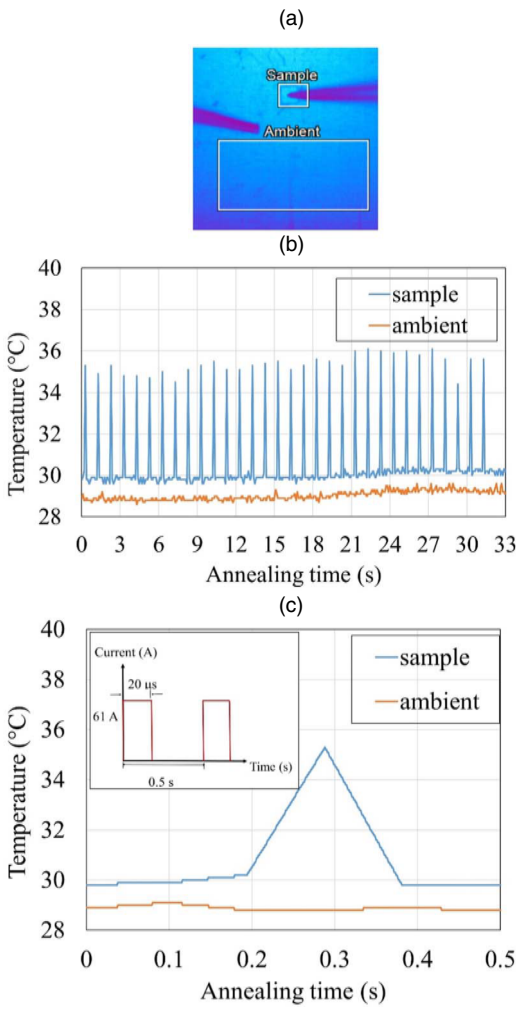

Fig. 1. (a) Thermal microscope image of diode during annealing; (b) temperature profile on diode surface and its surroundings; (c) the schematic of applied pulse (inset) and corresponding temperature rise due to a single pulse.

functionality. In the forward bias operation, it is observed that the pristine diode demonstrates the expected linear behavior after the turn-on voltage (Fig. 3). The forward current at 1.1 V of forward voltage is 104 mA. Post-degradation, the diode exhibits reduced forward current of 45 mA at the same forward voltage (1.1 V), suggesting an increase in series resistance or damage to the junction. After electropulsing, the forward current is 92 mA at 1.1 V of forward current, which revealed a marked restoration of forward current in the electropulsed diode, approaching the pristine diode's performance. Complementing this, the ideality factor analysis (Fig. 4) is provided to get further insights into the quality of the diode's junction. For an ideal diode, the ideality factor is 1, but real diodes typically have an ideality factor greater than 1, due to recombination and generation in the depletion region, series resistance, and other non-ideal effects.[37)]

The Shockley diode equation provides a mathematical model for the *I*–*V* characteristics of a diode.[14,38)] It states that the diode current "*I*" under forward bias is given by $I = I_0(e^{\frac{qV}{nKT}} - 1)$; where, I_0 is the reverse saturation current, q is the charge of an electron, V is the voltage across the diode, n is the ideality factor, k is the Boltzmann constant, and T is the absolute temperature. Rearranging this equation gives the slope of the ln(I) versus V curve as $\frac{q}{nKT}$, which is inversely proportional to the ideality factor n. For our analysis, ln(I) versus V curves were plotted [Fig. 4(a)], and the slopes for the pristine, degraded, and pulsed conditions within linear region were measured as approximately 32.84, 20.17, and 31.97, respectively. These values correspond to ideality factors of approximately 1.16 for the pristine, 1.92 for the degraded, and 1.20 for the pulsed diode. The intentional degradation may introduce additional trap states into the device, which are imperfections in the semiconductor lattice that capture charge carriers and lead to increased recombination in the depletion region,[12,13)] necessitating a higher forward voltage for the same current and resulting in a higher ideality factor of 1.92. Conversely, the reduction in the ideality factor for the pulsed diode to 1.20 suggests that the electropulsing treatment effectively reduced the recombination and thus defect density. Furthermore, we extended our investigation to include the local ideality factor, analyzing the diode's behavior over a higher voltage range [Fig. 4(b)]. This analysis revealed that across every voltage level, the ideality factor for the degraded diode remained consistently higher than that of the pristine and pulsed diodes. This confirms that

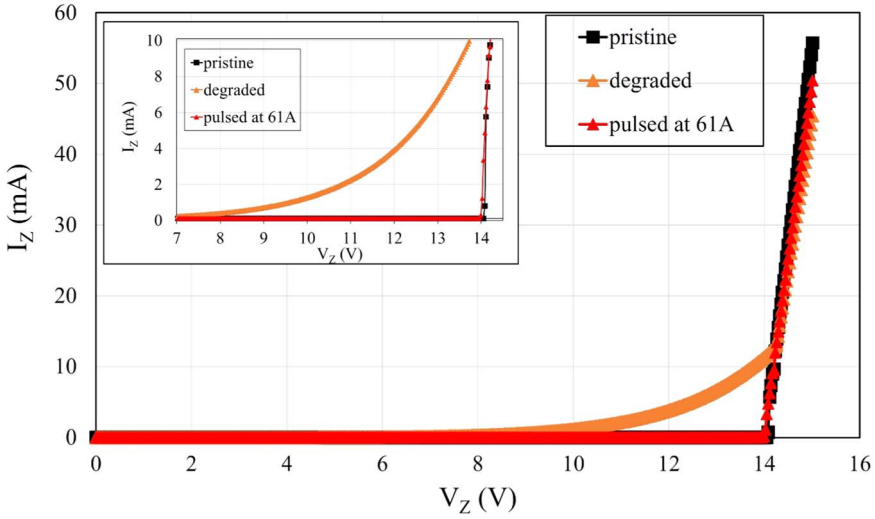

Fig. 2. *I*–*V* characteristic curves of Zener diode in various states of Zener-bias mode; inset provides a detailed comparison within the knee region of 7–14.5 V.

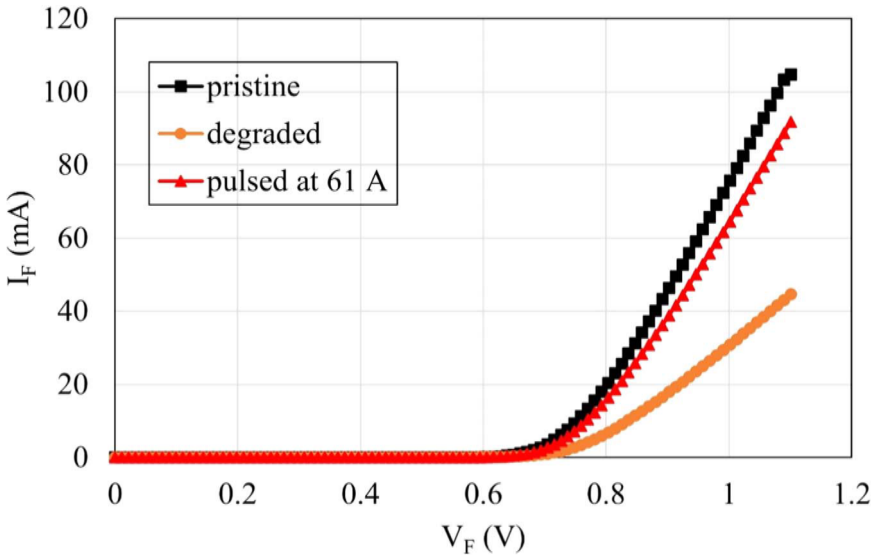

Fig. 3. *I–V* characteristic curves of Zener diode in various states of Forward-bias mode.

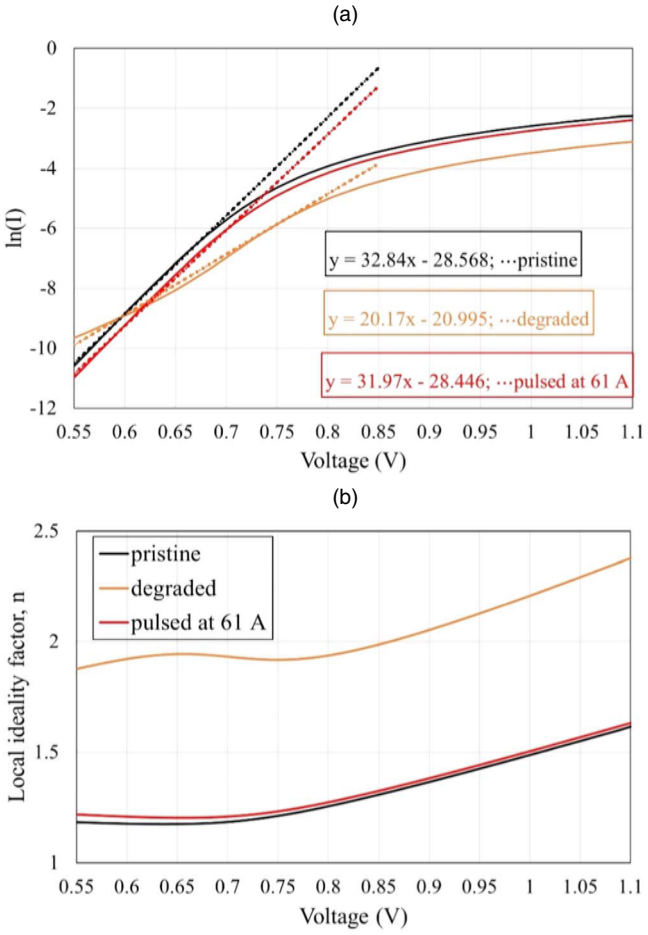

Fig. 4. (a) ln(*I*)–*V* characteristics for different states, (b) local ideality factor for various voltages.

the degradation process adversely affected the diode across its operational range, and that the non-conventional RT pulse treatment was successful in mitigating these effects, not only at a specific point but across a continuum of operational conditions.

The Raman spectra of a pristine Si Zener diode and one subjected to electropulsing treatment are conducted at two separate spatial locations to assess recovery in crystal quality (Fig. 5). The main graph shows the Raman peaks are centered around the characteristic silicon phonon mode near 520 (cm^{-1}).[39] In both positions, the intensity of the pulsed sample is higher than the pristine state. The insets provide a closer look at the normalized intensity to facilitate a direct comparison of the full width at half maximum (FWHM) for the two samples. For the pristine sample, the FWHM is measured to be 7.455 cm^{-1}, and post-electropulsing, we observe a decrease in the FWHM at one position to 5.445 cm^{-1} [Fig. 5(a)] and at another position to 6.768 cm^{-1} [Fig. 5(b)]. The observed reduction in FWHM in the pulsed sample corroborates that the electropulsing treatment has effectively annealed the crystal defects introduced during the degradation process.[40,41] Remarkably, the FWHM in the pulsed sample is even more narrow than that of the pristine sample, suggesting that the electropulsing not only reversed the damage but may have also enhanced the crystal quality beyond the initial state. However, the discrepancy in FWHM between two different locations on the pulsed sample (5.445 cm^{-1} versus 6.768 cm^{-1}) suggests that the recovery is spatially heterogeneous. This implies that while the overall trend points toward a structural recovery, it did not uniformly restore the diode's crystal structure across the entire sample. This non-uniformity in recovery process might result from the variations in the distribution of defects within the degraded diode leading to localized areas where the defect annihilation was less effective. One limitation in our study is the inability to provide Raman spectra for the degraded state of the diode due to the etching requirement for Raman analysis, which would render the diode unsuitable for subsequent electropulsing. This restriction prevents a direct comparison between the degraded and recovered states, leaving a gap in the full understanding of the electropulsing treatment's impact on the diode's microstructure. Despite this, the Raman analysis offers valuable evidence of the electropulsing treatment's efficacy, albeit with the caveat of spatial non-uniformity in the recovery process.

In this study, we explored the rejuvenation of a Zener diode following its degradation due to high electrical stress.

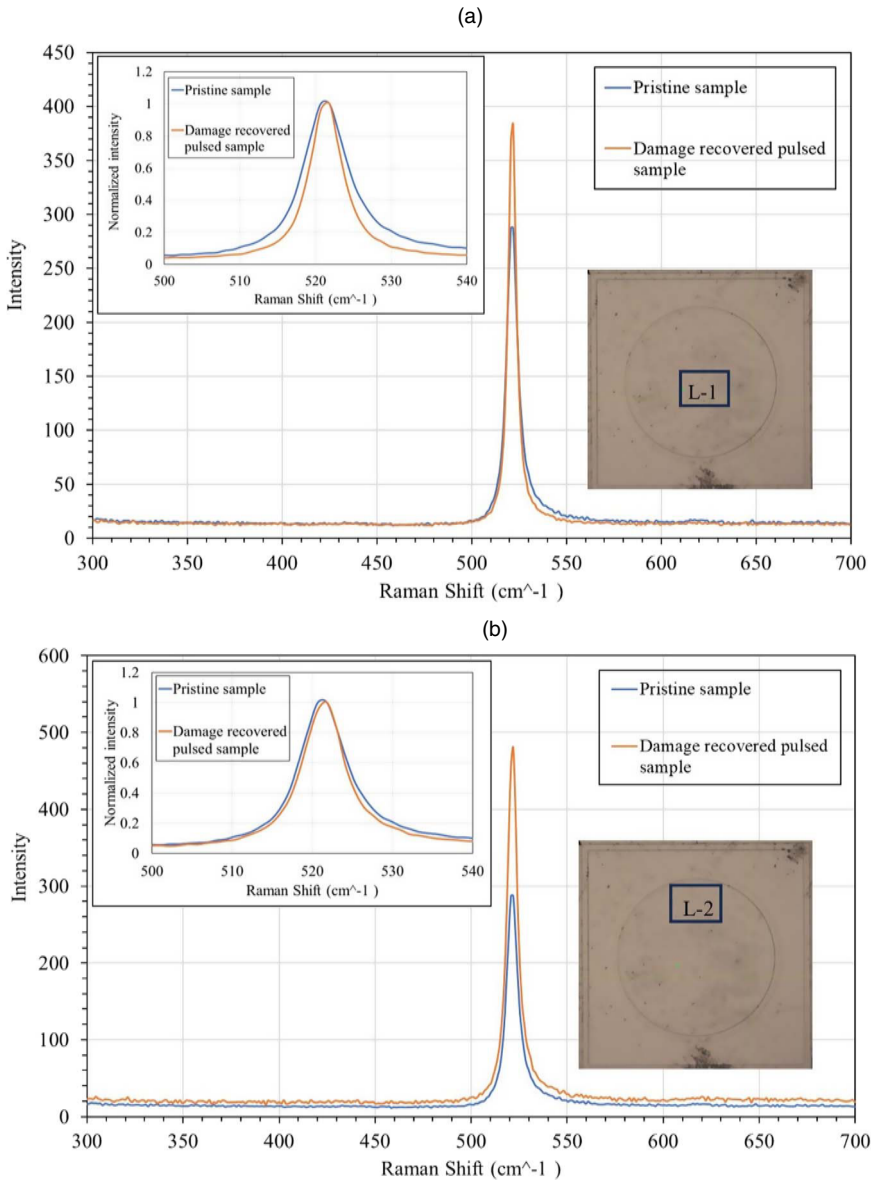

Fig. 5. Microanalysis using Raman spectroscopy; (a) at spatial location 1, and (b) at spatial location 2; L-1 and L-2 represent two distinct locations on diode at which Raman spectra have been collected; the left inset shows normalized intensity to compare the FWHM.

The stress resulted in a significant broadening and leftward shift of the Zener breakdown voltage knee, along with a 57% decrease in forward current. Utilizing a RT EWF assisted annealing, characterized by high-density electric pulses with short pulse widths and low frequencies, we successfully rejuvenated the diode's electrical and structural properties. The treatment restored the breakdown knee and recovered the forward current to approximately 85% of its original value. In addition, the ideality factor of the diode, which had increased significantly due to degradation, showed a substantial improvement after the electropulsing treatment, approaching the levels observed in the pristine diode. This suggests a successful reduction in defect-related non-ideal behaviors in the diode. Furthermore, structural analysis through Raman spectroscopy revealed a decrease in the FWHM, with values changing from 7.455 cm^{-1} in the pristine state to 5.445 cm^{-1} and 6.768 cm^{-1} at two distinct locations in the pulsed sample. This reduction in FWHM indicates an improvement in the crystalline structure of the diode, signifying a reduction in defect density/trap states formed due to the degradation process. However, the spatial variation in FWHM across the diode highlights the non-uniform nature of the recovery process. This study demonstrates the potential of electropulsing as an efficient, RT alternative to traditional thermal annealing methods for repairing electrically stressed semiconductors.

Acknowledgments We acknowledge the funding support from the US National Science Foundation (DMR # 2103928). The study was partially supported by the Defense Threat Reduction Agency (DTRA) as part of the Interaction of Ionizing Radiation with Matter University Research Alliance (IIRM-URA) under contract number HDTRA1-20-2-0002. N.G. acknowledges support from Air Force Office of Scientific Research under Award No. FA9550-19RYCOR050. The views expressed in the article do not necessarily represent the views of the United States Government.

ORCID iDs Md Hafijur Rahman https://orcid.org/0000-0002-1440-1839 Aman Haque https://orcid.org/0000-0001-6535-5484 Stephen Pearton https://orcid.org/0000-0001-6498-1256

1) D. Neamen, *Semiconductor Physics and Devices : Basic Principles* (McGrawHil, New York, 2003).
2) O. N. Acosta, IEEE Trans. Ind. Gen. Appl. **IGA-5**, 481 (1969).

3) V. Bucur, G. Banarie, S. Marinca, and M. Bodea, "A Zener-Based Voltage Reference Design Compensated Using a ΔVBE Stack," 2018 25th Int. Conf. "Mixed Design of Integrated Circuits and System" (MIXDES), p. 116.
4) B. Setera and A. Christou, "Challenges of Overcoming Defects in Wide Bandgap Semiconductor Power Electronics," Electronics **11**, 10 (2022).
5) N. S. Weingarten and P. W. Chung, Scr. Mater. **69**, 311 (2013).
6) J. P. Hirth and J. Lothe, *Theory of Dislocations* (Krieger Publishing Company, Malabar, FL, USA, 1992).
7) A. Tanaka et al., J. Appl. Phys. **125**, 82517 (2018).
8) S. Nakamura and S. Okamoto, IEEE Trans. Nucl. Sci. **42**, 102 (1995).
9) Z. Islam et al., Microelectron. Reliab. **102**, 113493 (2019).
10) T. Kimoto et al., ECS Trans. **50**, 25 (2013).
11) R. Myers-Ward et al., ECS Trans. **50**, 103 (2013).
12) J. R. Nicholls, Microelectron. Reliab. **127**, 114386 (2021).
13) S. U. Omar, T. S. Sudarshan, T. A. Rana, H. Song, and M. V. S. Chandrashekhar, IEEE Trans. Electron Devices **62**, 615 (2015).
14) E. H. Rhoderick and R. H. Williams, *Metal–Semiconductor Contacts* (Clarendon, Oxford, 1988).
15) M. Sochacki, A. Kolendo, J. Szmidt, and A. Werbowy, Solid State Electron. **49**, 585 (2005).
16) S. K. Gupta, A. Azam, and J. Akhtar, Phys. B Condens. Matter **406**, 3030 (2011).
17) M. A. Mannan, K. V. Nguyen, R. O. Pak, C. Oner, and K. C. Mandal, IEEE Trans. Nucl. Sci. **63**, 1083 (2016).
18) N. M. Shmidt et al., Phys. Status Solidi **216**, 533 (1999).
19) D. H. Kim et al., Solid State Phenomena **124-126**, 105 (2007).
20) S. B. Yun et al., J. Nanosci. Nanotechnol. **17**, 3406 (2017).
21) M. Ohring, *The Materials Science of Thin-films* (Academic, New York, 1992).
22) L. Freund and S. Suresh, *Thin Film Materials: Stress, Defect Formation, and Surface Evolution* (Cambridge University Press, Cambridge, England, 2003).
23) M. Szala, G. Winiarski, Ł. Wójcik, and T. Bulzak, Materials **13**, 2022 (2020).
24) X.-Q. Zha et al., Mater. Res. Express **6**, 96506 (2019).
25) J. Wu, C. Liao, Y. Yang, G. Yang, and M. Wu, Metall. Mater. Trans. A **51**, 6759 (2020).
26) L. Xue et al., Mater. Res. Express **10**, 66513 (2023).
27) H. Song et al., Mater. Res. Express **7**, 66512 (2020).
28) M. A. J. Rasel et al., Appl. Phys. Lett. **122**, 204101 (2023).
29) M. A. J. Rasel et al., ECS J. Solid State Sci. Technol. **11**, 75002 (2022).
30) M. H. Rahman, H. Oh, D. Waryoba, and A. Haque, Mater. Res. Express **10**, 116521 (2023).
31) A. Haque, J. Sherbondy, D. Warywoba, P. Hsu, and S. Roy, J. Mater. Process. Technol. **299**, 117391 (2022).
32) A. Yamaguchi et al., Appl. Phys. Lett. **86**, 12511 (2004).
33) J. Lienig and M. Thiele, *Fundamentals of Electromigration-aware Integrated Circuit Design* (Springer, Cham, 2018), 10.1007/978-3-319-73558-0.
34) V. Sopko, B. Sopko, D. Chren, and J. Dammer, Nucl. Instrum. Methods Phys. Res., Sect. A **730**, 146 (2013).
35) M. H. Rahman, N. Glavin, A. Haque, F. Ren, and S. J. Pearton, ECS J. Solid State Sci. Technol. **13**, 25003 (2024).
36) M. H. Rahman, S. Todaro, L. Warner, D. Waryoba, and A. Haque, Metals **14**, 331 (2024).
37) M. A. Kroon and R. A.-C. M. M. van Swaaij, J. Appl. Phys. **90**, 994 (2001).
38) W. Shockley, Bell Syst. Tech. J. **28**, 435 (1949).
39) S. Narayanan, S. Kalidindi, and L. Schadler, J. Appl. Phys. **82**, 2595 (1997).
40) K. Kitahara, T. Ishii, J. Suzuki, T. Bessyo, N. Watanabe, and J. Zhang, Int. J. Spectrosc. **2011**, 632139 (2011).
41) K. Niwase and M. S. Amer, Int. J. Spectrosc. **2012**, 197609 (2012).